JOURNAL OF MATERIALS SCIENCE 23 (1988) 3981–3986

Thin films of molybdenum and tungsten disulphides by metal organic chemical vapour deposition

WOLFGANG K. HOFMANN
Hahn-Meitner-Institut Berlin, Bereich Strahlenchemie, Glienicker Str. 100, 1000 Berlin 39, FRG

Thin films of MoS_2 and WS_2 have been prepared on various substrates (glass, quartz, LiF, MgO, mica, molybdenum, gold, platinum, aluminium, copper, steel, graphite, $MoSe_2$) by metal-organic chemical vapour deposition using sulphur or hydrogen sulphide and the hexacarbonyls of the transition metals as volatile components. The deposition technique is described here. The thin layers have been examined by X-ray powder diffraction and scanning electron microscopy. Time-resolved microwave conductivity measurements were used to detect the photoactivity of these materials.

1. Introduction

The disulphides of molybdenum and tungsten, MoS_2 and WS_2, crystallize with a layer-type structure [1]; they are semiconductors, have high absorptivities and corrosion-resistance, and their band-gaps lie in the optimum range for solar energy conversion [2–4]. MoS_2 is also one of the most widely used solid lubricants which maintains its lubricating properties over large ranges of pressure and temperature [5]. The molybdenum and tungsten dichalcogenides can be prepared as single crystals by halogen vapour transport (HVT) [6], vapour growth (VG) [7] or flux growth [8]; thin layers of these compounds have been synthesized by radio-frequency sputtering [9, 10] and chemical vapour deposition (CVD) [11] using the hexafluorides as volatile metal compounds. Many successful attempts have been made to develop thin films of the refractory metals molybdenum and tungsten [12, 13]. The starting components in these cases are the hexafluorides or the hexacarbonyls of the metals. This paper reports a new metal-organic chemical vapour deposition (MOCVD) technique to grow thin films of MoS_2 and WS_2 on different kinds of substrate such as glass, metals and single crystals using the hexacarbonyls $M(CO)_6$ of the metals and H_2S and sulphur as starting components.

2. Experimental procedure

2.1. Preparation of thin layers

Thin MoS_2 and WS_2 films were deposited on various substrates (glass, quartz, mica, steel, graphite, LiF, MgO, $MoSe_2$ crystals, copper, gold, platinum, molybdenum, aluminium). A vertical reactor with flowmeters for the carrier gas (argon) and hydrogen sulphide was used. The MOCVD reactor consists of glass and is shown in Fig. 1. A graphite cylinder (diameter 22 mm, length 35 mm) acted as a holder for the substrates (diameter 20 mm) and was r.f. heated (model no. hfa 80 Koppold). The argon carrier gas had a stated purity of 4N8 : 99.998%, the the H_2S source 2N8 : 99.8% and the sulphur (Ventron) of m6n : 99.9999%. The starting materials for the metal component $Mo(CO)_6$ (Ventron) and $W(CO)_6$ (Aldrich) had stated purities of 99%.

The growth conditions for thin layers of MoS_2 and WS_2 are summarized in Table I. The glass substrates were etched for 5 min in a mixture of $HF : H_2SO_4 : H_2O = 1 : 3 : 1$, washed with distilled water and dried under N_2. The other substrates were cleaned with trichlorethylene. The reactor was set up under argon. When the substrate and the volatile starting components had reached the desired temperatures, the decomposition and film formation took place immediately. The synthesized MoS_2 and WS_2 sheets remained in the reactor for about half an hour and were cooled to room temperature in an argon atmosphere. The deposition temperature was varied in the range of 150 to 400° C and different gas flow rates were used (Table I). The hexacarbonyls were sublimated (100 to 200° C) and transported to the substrate by the carrier gas. Saturated solutions of the carbonyls in toluene have also been used as metal sources (solution-assisted MOCVD).

A quartz reactor was illuminated with a xenon UV lamp in order to weaken the chemical bonds in the carbonyls and H_2S, thus making the deposition easier or at least to visualize the flow patterns in the reactor system (light-induced MOCVD). The reactor system could also be evacuated (reduced-pressure MOCVD); under reduced pressure the deposition rate decreased, but the coverage of the substrates was better and fewer turbulences occurred in the reactor.

2.2. Characterization of thin MoS_2 and WS_2 layers

The surface morphology and growth direction of the thin layers was examined in a scanning electron

0022-2461/88 $03.00 + .12

TABLE I Growth conditions for $MoS_2(WS_2)$ thin films by MOCVD

No.	Compound	Substrate temp. (°C)	Source temp. (°C)		Gas flow rate ($l\,min^{-1}$)				Substrate	MOCVD technique	Remarks
			$M(CO)_6$	S	$Ar(H_2S)(S)$	Argon carrier gas	$Ar(M(CO)_6)$	H_2S			
1	MoS_2	200	100	–	2.5	0.8	0.8	0.3	Glass	–	Black, like velvet
2	WS_2	300	100	–	2.5	0.8	0.8	0.3	Glass	Atmospheric pressure	Brown, transparent
3	$Mo_xW_{1-x}S_2$	250	100	–	2.5	0.8	0.8	0.3	Glass	–	Grey
4	MoS_2	350	300	–	4.7	1.9	1.9	0.9	Glass	Solution-assisted	–
5	MoS_2	250	300	–	5.6	1.8	1.8	1.1	Glass	Light-induced	Turbulences
6	MoS_2	300	200	–	6.5	1.9	1.9	1.7	Glass	Reduced pressure	Better coverage than under atmospheric pressure
7	MoS_2	300	200	–	6.5	1.9	1.9	1.7	Quartz		
8	MoS_2	175	100	–	7.0	1.0	1.0	1.0	Mica	Atmospheric pressure	–
9	MoS_2	275	200	–	7.0	1.3	1.3	1.5	MgO		–
10	MoS_2	275	200	–	7.0	1.3	1.3	1.5	LiF		Good coverage
11	MoS_2	275	200	–	7.0	1.0	1.0	1.1	Mo		Good coverage
12	MoS_2	200	150	–	4.3	1.8	1.8	0.9	Al		Good coverage
13	MoS_2	300	200	–	3.5	1.5	1.5	0.9	Au		Good coverage
14	MoS_2	350	200	–	5.6	1.5	1.5	0.9	Pt		Good coverage
15	MoS_2	250	200	–	2.8	1.5	1.5	0.7	Cu		Good coverage
16	MoS_2	300	150	–	5.6	1.5	1.7	0.9	$MoSe_2$		Grey film on the silvery substrate
17	MoS_2	300	250	–	2.8	1.5	1.5	0.7	Steel		–
18	MoS_2	350	250	–	5.0	1.8	1.8	0.9	Graphite		–
19	MoS_2	350	150	300	4.0	1.0	1.0	–	Glass		Black
20	MoS_2	250	100	–	2.0	1.2	1.2	1.1	Mo	Light-induced, Reduced pressure	

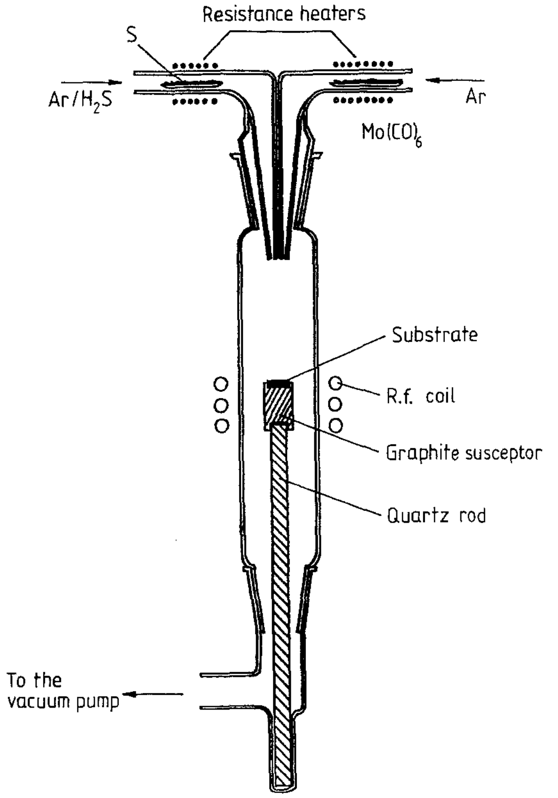

Figure 1 Vertical MOCVD reactor.

microscope (Cambridge Instruments 250 MK3) and the composition of the samples was analysed by microprobe analysis with an energy-dispersive system (EDAX). X-ray powder diffractograms were recorded with Cu*Kα* radiation using a Philips powder diffractometer. The thickness of the films was determined with a Sloan surface-profile measuring system. The photoactivity of the thin sheets was measured by the time-resolved microwave conductivity (TRMC) method. This method allows contactless measurements of the light-induced excess carrier absorption. The TRMC signals were induced by 532 nm light pulses of an Nd–YAG laser; the method is based on the proportionality between the relative change of the reflected microwave power upon illumination and the induced conductivity [14, 15]. In addition, the temperature dependence of the d.c. conductivity of the films was measured in the range of 100 to 400 K. The sheets were contacted with silver–epoxy and placed in an evacuated chamber for heating or cooling; the temperature was controlled by a calibrated resistor. The conductivity was determined from the current flow under voltage bias.

3. Results and discussion

3.1. Surface morphology, grain size and growth behaviour

Thin sheets (0.5 to 1 μm) of MoS_2, WS_2 and $Mo_xW_{1-x}S_2$ ($0 \leqq x \leqq 1$) could be prepared on different kinds of substrates such as glass, metals and single crystals with the MOCVD technique at moderate temperatures according to the equations

$$M(CO)_6 + 2H_2S = MS_2 + 6CO + 2H_2 \quad (1)$$

$$M(CO)_6 + 2S = MS_2 + 6CO \quad (2)$$

where M = Mo, W. The X-ray powder diffractograms (Fig. 2) of the thin layers showed at least three peaks which were in good agreement with the expected powder patterns for molybdenite and tungstenite (MoS_2 and WS_2) which were calculated with the Lazy Pulverix program [16]. The diffraction peaks were slightly broadened indicating small crystal size. The average grain size of the deposited layers could be determined using Scherrer's equation [17]:

$$D = K\lambda/\beta \cos\theta \quad (3)$$

where D = mean dimension of the crystallite perpendicular to the hkl diffraction planes, K = constant = 0.9 (see also [18]), λ = wavelength, β = half maximum peak width and θ = Bragg angle. This gives a relationship between the grain size of the crystals and X-ray line broadening. Using the diffraction peaks (0 0 2)(2θ = 14.05°) and (1 0 0)(2θ = 32.80°) an average grain size between 6.0 and 7.5 nm was calculated.

The intensities for the (0 0 l) diffraction planes are much lower than expected from the calculated powder patterns [16]. This is due to a texture effect. Most of the MS_2 (M = Mo, W) crystals are not orientated parallel to the substrates. As one can see from the scanning electron micrographs (Fig. 3), the films exhibit a lamellar microstructure type with the (0 0 2) planes of the MS_2 crystallites perpendicular to the substrates. The basal planes perpendicular to the surface of the substrates are randomly orientated and large agglomerates of MS_2 crystals are formed, looking like a cauliflower (Fig. 3d). The layer-type structure is highly anisotropic and the fastest growing area (0 0 2) is oriented in the direction of lower tem-

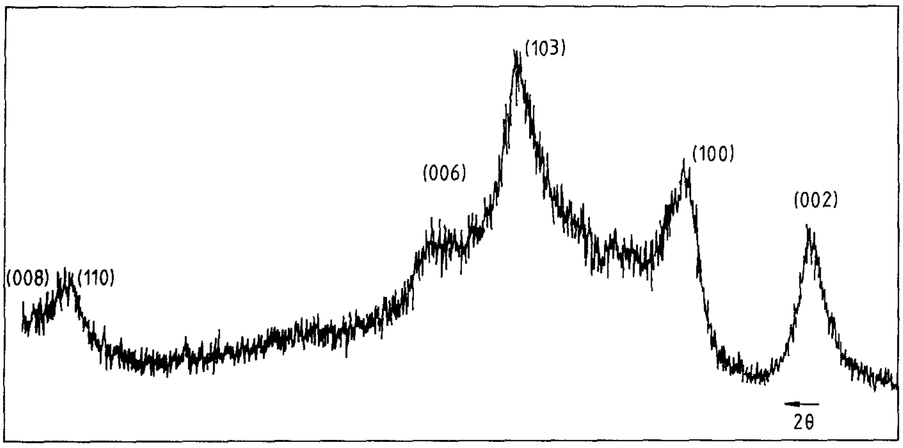

Figure 2 X-ray diffractogram of a WS_2 layer deposited on glass (Cu*Kα* = 0.15418 nm).

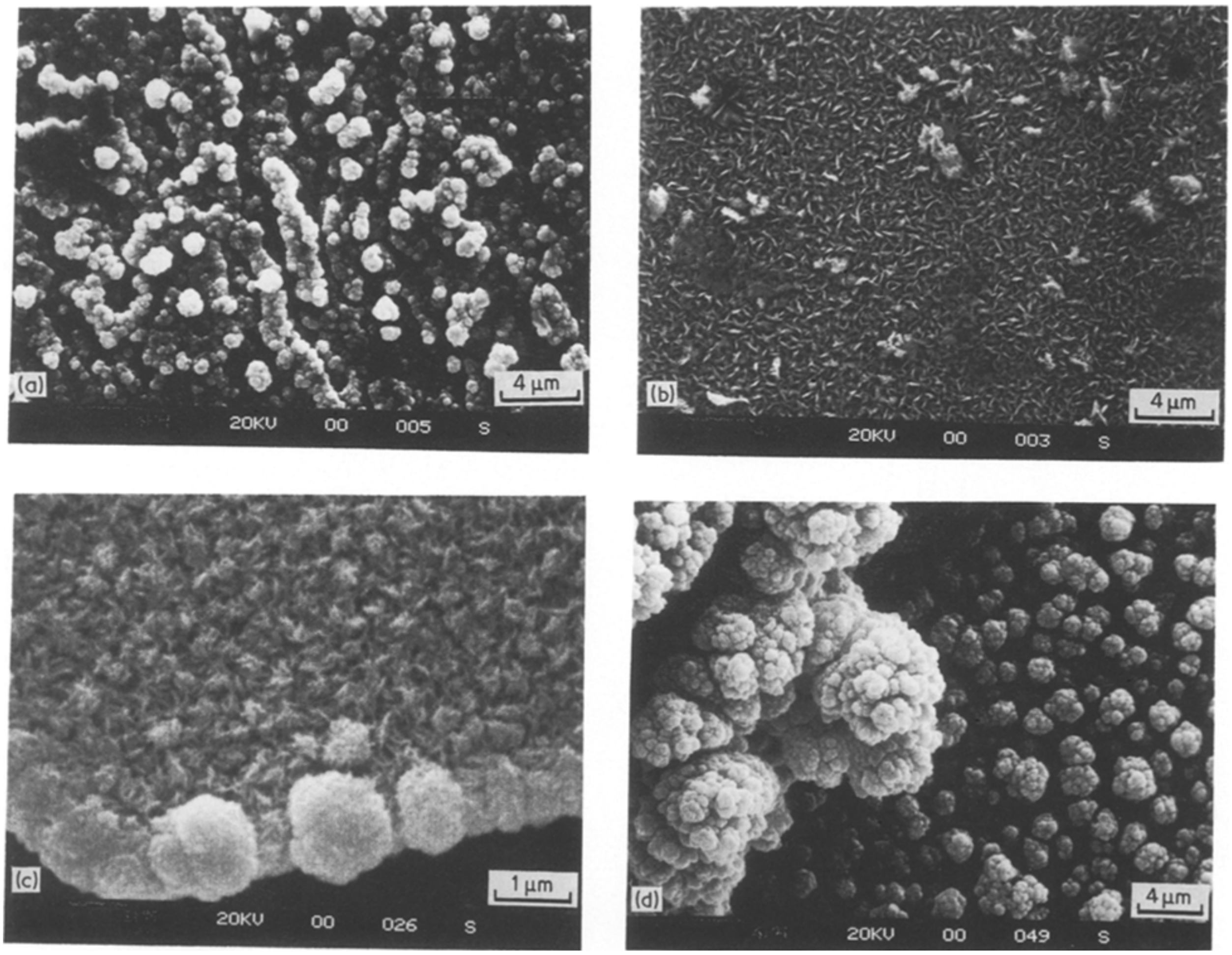

Figure 3 Scanning electron micrographs of thin films of MoS_2 on different substrates. (a) MoS_2 deposited on molybdenum, $E_B = 20\,kV$ (MOCVD, solution-assisted); (b) MoS_2 deposited on glass, $E_B = 20\,kV$ (MOCVD, reduced pressure); (c) MoS_2 deposited on $MoSe_2$ (CVT), $E_B = 20\,kV$; (d) MoS_2 deposited on platinum, $E_B = 20\,kV$.

perature. This irregular growth behaviour was observed in all the MOCVD experiments performed here. The use of reduced pressure, for instance, or the nature of the substrate (even $MoSe_2$ CVT, chemical vapour transport crystals) seemed to have no influence. No crystal growth parallel to the surface of the substrates could be detected. A growth mechanism with the crystals randomly distributed over the surface of the substrates with their basal plane (0 0 2) perpendicular to the substrate was observed for r.f.-sputtered MoS_2 samples [19], as well as for layers of WSe_2 reactively sputtered or chemical-vapour-deposited using WF_6 as volatile metal compound and H_2 as carrier gas [11]. Only two experiments are known to have resulted in thin layers parallel to the substrate. An ultrathin (0.7 nm) layer of $MoSe_2$ parallel to an MoS_2 crystal as substrate was grown in an molecular beam epitaxy (MBE) chamber by Van der Waals epitaxy [20], and in the case of $MoTe_2$ it is possible to get thin films parallel to the surface of different substrates by d.c. diode sputtering and post-annealing in a tellurium atmosphere [21].

The main parameter in MOCVD is the temperature of the substrate. If it is too low, no deposition will occur; if it is too high, the quality of the layers is reduced because of the decomposition and re-evaporation of the deposited substances. In the temperature range used here (150 to 450° C), no clear relationship between substrate temperature, film thickness, grain size and crystal orientation could be observed. All the layers showed a disordered distribution of the MoS_2 crystallites regardless of the substrate used, and the crystal size did not vary much with substrate temperature or amount of carrier gas.

The composition of the thin layers was examined by EDAX equipment attached to the scanning electron microscope. The analysis of MoS_2 samples is difficult because of the complete overlap of the SK_α and $MoL\alpha$ peaks. The composition of MoS_2 would therefore not be measured with sufficient accuracy. This is not the case in the analysis of WS_2 samples prepared under similar conditions, which resulted in the expected values for an MX_2 compound (Fig. 4).

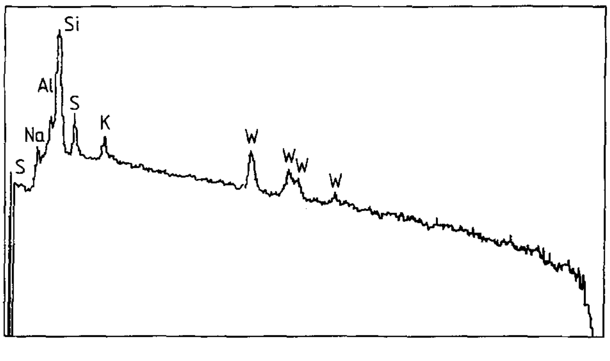

Figure 4 EDAX pattern of a WS_2 layer deposited on glass.

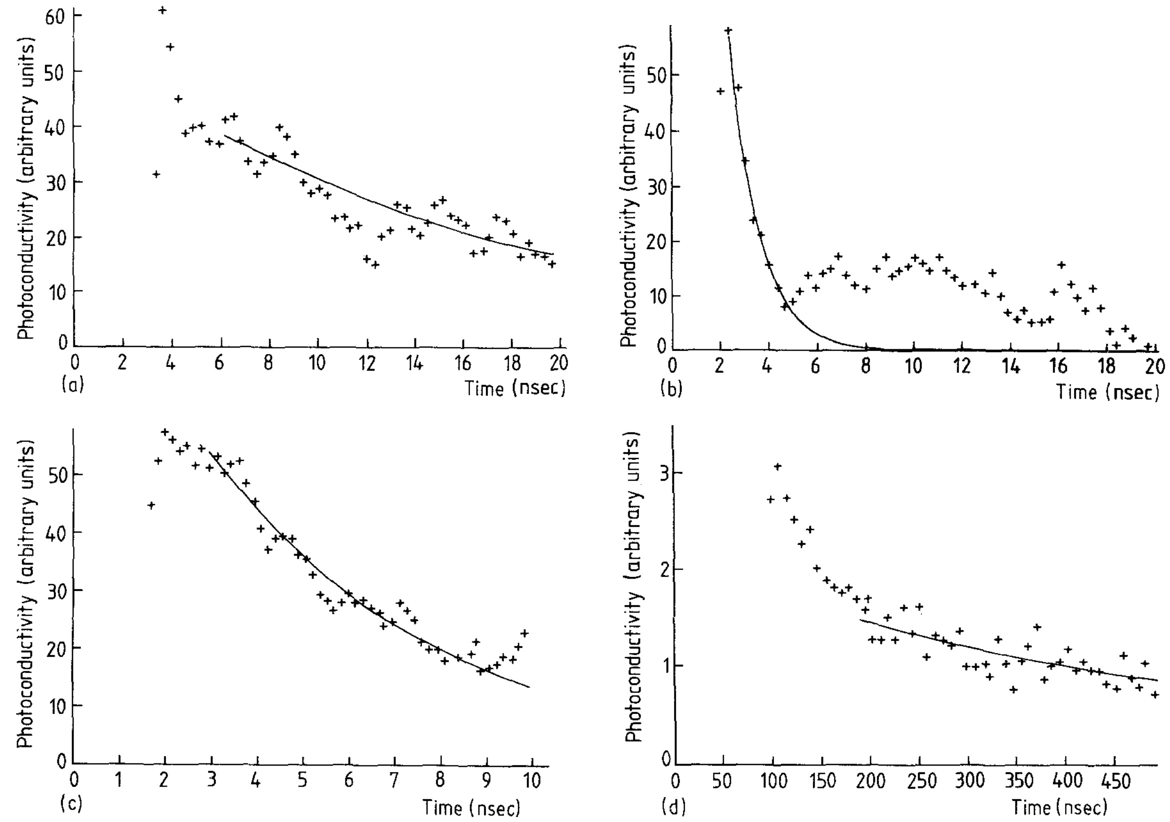

Figure 5 Light-induced excess microwave conductivity transients for MoS_2 films (illumination Nd-YAG laser, λ = 530 nm). (a) MoS_2 on glass, (b) $Mo_xW_{1-x}S_2$ on glass, (c) MoS_2 deposited on glass, (d) MoS_2 deposited on mica.

3.2. Time-resolved microwave conductivity and d.c. conductivity measurements

The photoactivity of the thin MS_2 layers was detected with TRMC measurements. In the case of WS_2 films no change of the reflected microwave signal was observed; the MoS_2 layers, however, were photoactive as indicated by the characteristic features of the microwave signal (Fig. 5). The peak height is related to the amount of induced charge carriers and the decay of the curve depends on the lifetime of the generated charge carriers. For the layers with mixed compositions $Mo_xW_{1-x}S_2$ ($0 \leqq x \leqq 1$) the photoactivity is lower than for the pure MoS_2 films; with decreasing x (increasing amount of tungsten within the sheets) the intensity of the microwave signal decreases. Figs 5a and b show the microwave conductivities of MoS_2 and $Mo_xW_{1-x}S_2$ samples. The peak height of the $Mo_xW_{1-x}S_2$ sample is considerably lower than the peak height in the pure MoS_2 sample. The lower photoactivity of WS_2 samples compared to MoS_2 is also observed when polycrystalline powders or single crystals of these materials are examined with the TRMC technique. In Figs 5c and d the microwave transients of two MoS_2 samples deposited on different substrates (glass and mica) are compared to each other. The decay of the microwave signal of the MoS_2 film deposited on glass is much steeper than the decay of the curve for MoS_2 on mica. So the lifetime of the charge carriers in MoS_2 deposited on mica is higher than on samples prepared on glass. Metallic substrates could not be examined with the microwave technique.

The amount of $Mo(CO)_6$ used in the preparation of MoS_2 MOCVD layers determines the conductivity of the sample. This could be observed from the TRMC measurements of MoS_2 sheets prepared under similar conditions with varying $Mo(CO)_6/H_2S$ ratios. Excess $Mo(CO)_6$ causes a high intrinsic conductivity and almost metallic behaviour; with lower amounts of $Mo(CO)_6$ the samples become photoactive.

The temperature dependence of the conductivity was measured for differently prepared samples. Here an almost metallic behaviour (Fig. 6) was observed. With the TRMC technique the photoactivity of some crystallites within the thin layers could be detected, whereas the d.c. conductivity measurements describe the electric properties of the whole layer.

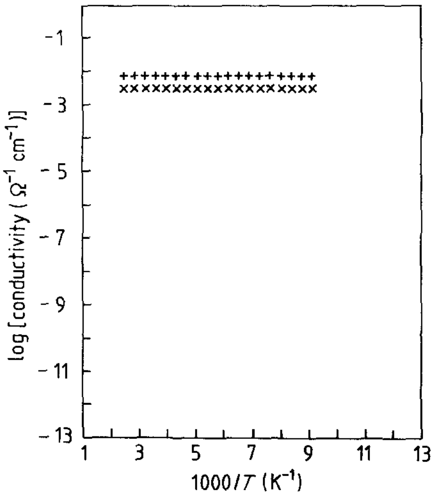

Figure 6 Temperature dependence of d.c. conductivity of MoS_2 films deposited on glass. (+) Pure sulphur as source, (x) H_2S as source of sulphur.

4. Conclusions

Thin layers of MoS_2, WS_2 and $Mo_xW_{1-x}S_2$ ($0 \leqq x \leqq 1$) were prepared by MOCVD under atmospheric conditions or reduced pressure with $M(CO)_6$, sulphur and/or H_2S as volatile components using different kinds of substrates such as glass, metals or single crystals in a vertical reactor. The films were examined by X-ray diffractometry, scanning electron microscopy and time-resolved microwave conductivity measurements. In all cases the MS_2 crystals grew with the basal plane perpendicular to the substrate. The TRMC measurements indicated that the MoS_2 layers were photoactive. However, as long as growth does not occur parallel to the surface of the respective substrate, these layers might not be applicable for solar energy conversion. There are, however, other applications possible, in particular in the field of energy storage where an irregular growth could be advantageous. The resulting enlarged surface area might allow good storage efficiency.

Acknowledgements

I wish to thank Priv.-Doz. Dr H. J. Lewerenz for critical reading of the manuscript. For the TRMC measurements I have to thank Dr M. Kunst and for the conductivity measurements Dr R. Könenkamp. The work was supported by the BMFT within Project No. RAC/DS 59042.

References

1. O. GLEMSER, H. SAUER and P. KÖNIG, *Z. Anorg. Chem.* **257** (1948) 241.
2. H. TRIBUTSCH, *Faraday Discuss. Chem. Soc.* **70** (1980) 189.
3. *Idem, Ber. Bunsenges. Phys. Chem.* **81** (4) (1977) 361.
4. *Idem, J. Electrochem. Soc.* **107** (1978) 1087.
5. T. SPALVINS, *Thin Solid Films* **96** (1982) 17.
6. H. BRIXNER, *J. Electrochem. Soc.* **110** 289 (1963).
7. A. A. AL-HILLI and B. L. EVANS, *J. Crystal Growth* **15** (1972) 93.
8. W. K. HOFMANN, *ibid.* **75** (1986) 93.
9. R. BICHSEL, P. BUFFAT and F. LEVY, *J. Phys. D: Appl. Phys.* **19** (1986) 1575.
10. Th. B. STEWART and P. D. FLEISCHAUER, *Inorg. Chem.* **21** (1982) 2426.
11. D. E. MILLER, "Development of Tungsten Selenide Thin Films for Photovoltaics", Report No. URCL-53665 (Lawrence Livermore National Laboratory, University of California, 1985).
12. L. H. KAPLAN and F. M. d'HEURLE, *J. Electrochem. Soc.* **117** (1970) 693.
13. W. R. HOLMAN and F. J. HUEGEL, *J. Vac. Sci. Technol.* **11** (4) (1974) 701.
14. M. KUNST and H. TRIBUTSCH, *Chem. Phys. Lett.* **105** (1984) 123.
15. M. KUNST and A. WERNER, *J. Appl. Phys.* **58** (1985) 2236.
16. K. YVON, W. JEITSCHKO and E. PARTHÉ, *J. Appl. Crystallogr.* **10** (1977) 73.
17. P. SCHERRER, *Göttinger Nachr.* **2** (1918) 98.
18. S. F. BARTRAM, in "Handbook of X-Rays", edited by E. F. Kaelbe (McGraw-Hill, New York, 1967) ch. 17.
19. R. BICHSEL and F. LÉVY, *J. Phys. D: Appl. Phys.* **19** (1986) 1809.
20. A. KOMA, K. SUNOUCHI and T. MIYAJIMA, *J. Vac. Sci. Technol.* **B3** (1985) 724.
21. J. C. BERNEDE, M. KETTAF, A. MALLOUKY and R. MESSOUSSI, in Proceedings of International Symposium on Trends and New Applications in Thin Films, Strasbourg, March 1987, (Laboratoire de Physique des Matériaux et Composants de l'Electronique, 2 Rue de la Houssinière, 44072, Nantes, France) Vol. 1, p. 21.

Received 29 October 1987
and accepted 25 February 1988